Immunity
Article

microRNA-155 Regulates the Generation of Immunoglobulin Class-Switched Plasma Cells

Elena Vigorito,[1,*] Kerry L. Perks,[3] Cei Abreu-Goodger,[4] Sam Bunting,[2] Zou Xiang,[5] Susan Kohlhaas,[1] Partha P. Das,[6] Eric A. Miska,[6] Antony Rodriguez,[4] Allan Bradley,[4] Kenneth G.C. Smith,[5] Cristina Rada,[7] Anton J. Enright,[4] Kai-Michael Toellner,[3] Ian C.M. MacLennan,[3] and Martin Turner[1,*]
[1]Laboratory of Lymphocyte Signalling and Development
[2]Laboratory of Chromatin and Gene Expression
The Babraham Institute, Cambridge, CB22 3AT, UK
[3]MRC Center for Immune Regulation, University of Birmingham, Birmingham, B15 2TT, UK
[4]The Wellcome Trust Sanger Institute, Wellcome Trust Genome Campus, Hinxton, Cambridge CB10 1SA, UK
[5]Cambridge Institute for Medical Research and the Department of Medicine, University of Cambridge School of Clinical Medicine, Box 139, Addenbrooke's Hospital, Cambridge, CB2 0XY, UK
[6]Gurdon Institute and Department of Biochemistry, University of Cambridge, Cambridge, CB2 1QN, UK
[7]Medical Research Council Laboratory of Molecular Biology, Hills Road, Cambridge CB2 2QH, UK
*Correspondence: elena.vigorito@bbsrc.ac.uk (E.V.), martin.turner@bbsrc.ac.uk (M.T.)
DOI 10.1016/j.immuni.2007.10.009

SUMMARY

microRNA-155 (miR-155) is expressed by cells of the immune system after activation and has been shown to be required for antibody production after vaccination with attenuated *Salmonella*. Here we show the intrinsic requirement for miR-155 in B cell responses to thymus-dependent and -independent antigens. B cells lacking miR-155 generated reduced extrafollicular and germinal center responses and failed to produce high-affinity IgG1 antibodies. Gene-expression profiling of activated B cells indicated that miR-155 regulates an array of genes with diverse function, many of which are predicted targets of miR-155. The transcription factor Pu.1 is validated as a direct target of miR155-mediated inhibition. When Pu.1 is overexpressed in wild-type B cells, fewer IgG1 cells are produced, indicating that loss of Pu.1 regulation is a contributing factor to the miR-155-deficient phenotype. Our results implicate post-transcriptional regulation of gene expression for establishing the terminal differentiation program of B cells.

INTRODUCTION

microRNAs (miRs) have been shown to regulate gene expression by sequence-specific base pairing, with target mRNAs initiating inhibition of translation or degradation of the mRNA. In animals, miRNAs are transcribed as primary miRNA (pri-miRNA). The pri-miRNA are processed in the nucleus to precursor miRNA (pre-miRNA) by the microprocessor complex prior to their transport into the cytoplasm. In the cytoplasm, they are further processed to mature miRNAs by Dicer and incorporated into the RNA-induced silencing complex (reviewed by Bartel, 2004). T cell-specific deletion of Dicer has revealed a role for this enzyme in thymic development and the differentiation of T lymphocytes (Cobb et al., 2005, 2006; Muljo et al., 2005; Neilson et al., 2007). Although these data imply that miRNAs may be important in lymphocyte development, essential functions for individual miRNAs have not yet emerged.

miR-155 is contained within the noncoding B cell integration cluster (*Bic*) gene (Lagos-Quintana et al., 2002). *Bic* was first identified as a frequent site of integration for the avian leukosis virus, and coexpression of bic with c-*myc* has been found to synergize for lymphomageneis (Tam et al., 1997). In humans, high expression of *BIC* and miR-155 has been shown in Hodgkin's lymphoma, primary mediastinal B cell lymphoma, and diffuse large B cell lymphoma, whereas very low expression of *BIC* and miR-155 were reported in adult Burkitt lymphoma (Eis et al., 2005; Metzler et al., 2004; van den Berg et al., 2003). When overexpressed as a transgene in B cells, miR-155 gives rise to pre-B cell lymphomas (Costinean et al., 2006). In untransformed cells of the immune system, Bic transcripts and miR-155 expression appear to be induced by antigenic stimulation (Haasch et al., 2002; Rodriguez et al., 2007). *Bic* is also expressed by macrophages after Toll-like receptor and type-I interferon stimulation (O'Connell et al., 2007) and in B cells after treatment with antibodies to surface IgM (van den Berg et al., 2003). Furthermore, a subset of human CD20-positive cells within the germinal center has been shown to express *BIC* by RNA in situ hybridization (van den Berg et al., 2003).

Previous studies show that miR-155 mutant mice display defective B and T cell immunity and abnormal function of antigen-presenting cells (Rodriguez et al., 2007; Thai et al., 2007). Moreover, a reduced number of germinal center B cells was observed in miR-155-deficient mice,

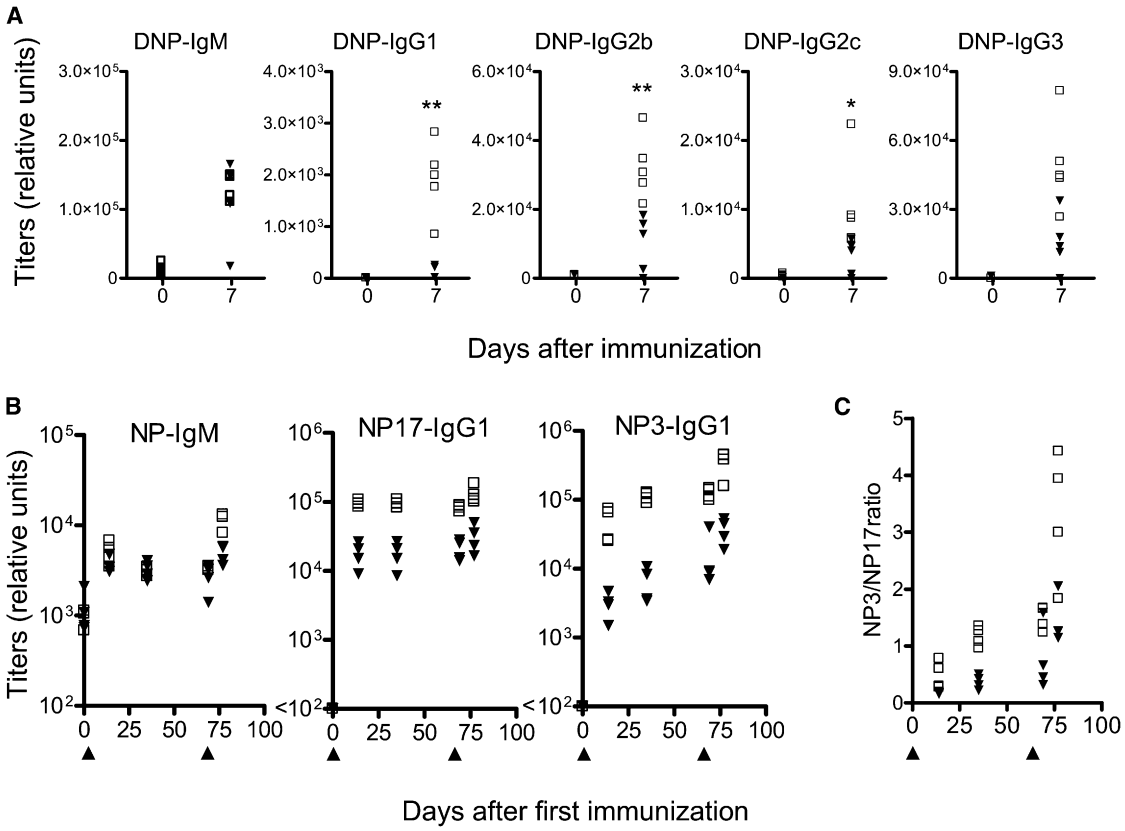

Figure 1. miR-155-Deficient Mice Produce Reduced Amounts of Low-Affinity IgG1 Antibodies

(A) Wild-type (open squares) or miR-155-deficient chimeric (filled triangles) mice were immunized with DNP-LPS, and anti-DNP-specific antibody titers were measured 7 days later. *$p < 0.05$; **$p < 0.005$ by Student's t test.

(B and C) Wild-type (open squares) or miR-155-deficient (filled triangles) mice were immunized with NP-KLH in alum at day 0 and day 70, indicated by the arrowheads. Production of NP-specific antibody titers were measured at the indicated times. Two-way ANOVA was performed and $p < 0.0001$ for the genotype and time effect for NP-specific IgG1 antibodies of low and high affinity. Similar experiments were done twice.

(B) Titers of IgM anti-NP were measured with NP_{17}-BSA (left). Titers of IgG1 anti-NP were measured with NP_{17}-BSA (middle) or NP_3-BSA (right).

(C) Ratio of the IgG1 titers detected with NP_3-BSA to those with NP_{17}-BSA. Each symbol corresponds to one mouse.

whereas its overexpression led to the opposite phenotype (Thai et al., 2007). Neither of these studies identified the cellular basis of the defects in vivo. Both studies used miR-155 germline mice, and the conditional expression of miR-155 was driven by Cre under the control of the CD21 promoter. Thus, expression of miR155 was targeted to both B cells and follicular dendritic cells (Victoratos et al., 2006). Here we show that defects in humoral immunity after primary and secondary immunization are intrinsic to B lymphocytes. Microarray analysis of B cells activated under conditions that promote class switching to IgG1 revealed that miR-155 regulates expression of many genes, a substantial fraction of which are predicted to be direct targets of miR-155. One of these genes was *Sfpi1* (encoding the transcription factor Pu.1), which has a highly conserved functional miR-155 binding site in its 3′UTR. Moreover, Pu.1 is highly expressed in miR-155-deficient B cells, and Pu.1 overexpression in wild-type B cells results in reduced numbers of IgG1-switched cells. Our results indicate that miR-155 plays a key role in antigen-driven B cell maturation and the persistence and/or differentiation of Ig class-switched cells and that deregulation of Pu.1 is likely to be a contributing factor to the phenotype observed in miR-155-deficient mice.

RESULTS

Deficiency in miR-155 Leads to Impaired Primary and Secondary Immune Response

It has been previously shown that miR-155 is dispensable for lymphocyte development but necessary for the generation of T and B cell responses in vivo (Rodriguez et al., 2007; Thai et al., 2007). To further understand the role of miR-155 in regulating the function of B cells, we studied the requirement of miR-155 for T-independent type-I (TI-1) responses by immunizing mice with the dinitrophenylated lypopolysaccharide (DNP-LPS). We observed defective switched antibody responses at day 7 after immunization (Figure 1A). By contrast, the production of antigen-specific IgM was normal.

Next we studied the response of miR-155-deficient mice to the well-characterized T-dependent (TD) antigen

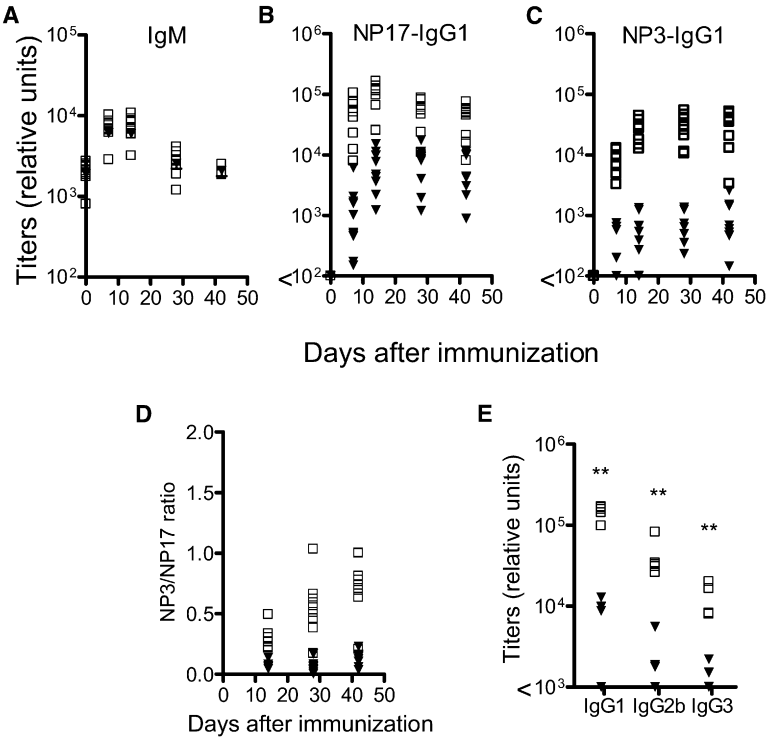

Figure 2. The Deficiency in Switched Antibody Production in miR-155-Deficient Mice Is B Cell Intrinsic

Wild-type (open squares) or miR-155-deficient (filled triangles) chimeras were immunized with NP-KLH in alum at day 0.

(A and B) Titers of IgM anti-NP (A) or IgG1 (B) were measured with NP_{17}-BSA.

(C) Titers of IgG1 anti-NP measured with NP_3-BSA.

(D) Ratio of the IgG1 titers detected with NP_3-BSA to those with NP_{17}-BSA.

(E) Titers of IgG1, IgG2b, and IgG3 anti-NP at day 14 after immunization. Each symbol corresponds to one mouse.

Statistical analysis: $p < 0.0001$ for the genotype and time effect of a two-way ANOVA analysis for (B)–(D). For (E), the Student's t test was used: $^{**}p < 0.001$. Similar experiments were done twice.

4-hydroxy-3-nitrophenylacetyl conjugated to keyhole limpet hemocyanin (NP-KLH). Wild-type and miR-155-deficient mice produced similar amounts of NP-specific antibodies of the IgM class after primary immunization (Figure 1B, left). On the other hand, the titers of primary IgG1 antibodies in miR-155 deficient mice were reduced to 20% of WT controls when NP_{17}-BSA was used as the capture antigen (Figure 1B, middle). With more stringent binding conditions with NP_3-BSA as the capture antigen, significant amounts of bound IgG1 were only seen in WT mice (Figure 1B, right), indicating impaired affinity maturation in the miR-155-deficient mice (Herzenberg et al., 1980). This defect can be readily seen by calculating the ratio of titers detected with NP_3-BSA to those of NP_{17}-BSA (Figure 1C). We also observed that reimmunization with soluble NP-KLH 70 days after primary immunization yielded impaired memory responses, suggesting that miR-155 is required for the generation and (or) maintenance or reactivation of memory B cells.

Deficiency in miR-155 Leads to Reduced IgG1 Secretion and Impaired Affinity Maturation in a B Cell-Autonomous Manner

We wished to determine whether the impaired antibody production was intrinsic to B cells. To this end, we created mixed chimeras by transferring 20% of either wild-type or miR-155-deficient bone-marrow cells with 80% of μMT-deficient bone-marrow cells into sublethally irradiated mice double deficient in *Rag2* and the common cytokine receptor gamma chain (*Rag2*$^{-/-}$ *Il2rg*$^{-/-}$ mice), as previously described (Huntington et al., 2006). The μMT mutation prevents the generation of B cells, so the B cells in the animals receiving miR-155-deficient marrow will be miR-155 deficient, whereas the recipients of wild-type marrow will have wild-type B cells. The 20/80 ratio favors reconstitution of all the other hemopoietic lineages from wild-type precursors (Huntington et al., 2006). Both groups of chimeras had similar proportions and numbers of B, $CD4^+$, and $CD8^+$ T cells (data not shown). We first studied the primary response to NP-KLH and found that the miR-155-deficient, μMT-deficient chimeras again had reduced IgG1 antibody production compared to the WT, μMT-deficient chimeras (Figures 2A–2D) and recapitulated the phenotype observed in miR-155-deficient mice: specifically, reduced amounts of NP-specific IgG1 in serum and impaired affinity maturation. We also observed that the defect in Ig secretion was not restricted to IgG1, because production of IgG2b and IgG3 subclasses was also significantly reduced ($p < 0.001$; Figure 2E). These results demonstrate a B cell-intrinsic requirement miR-155 for the production of switched and high-affinity antibodies.

Impaired Extrafollicular and Germinal Center Responses in the Absence of miR-155 Lead to Reduced Numbers of Antigen-Specific IgG1 AFC

The defects observed in the production of antigen-specific switched antibodies in response to NP-KLH prompted us to study the primary response by quantitative immunohistology. Immunization with T-dependent (TD) or T-independent (TI) antigens elicits an extrafollicular response that rapidly produces large amounts of IgM and switched antibodies providing a first line of defense. TD antigens, in addition, promote B cell growth in follicles where they form

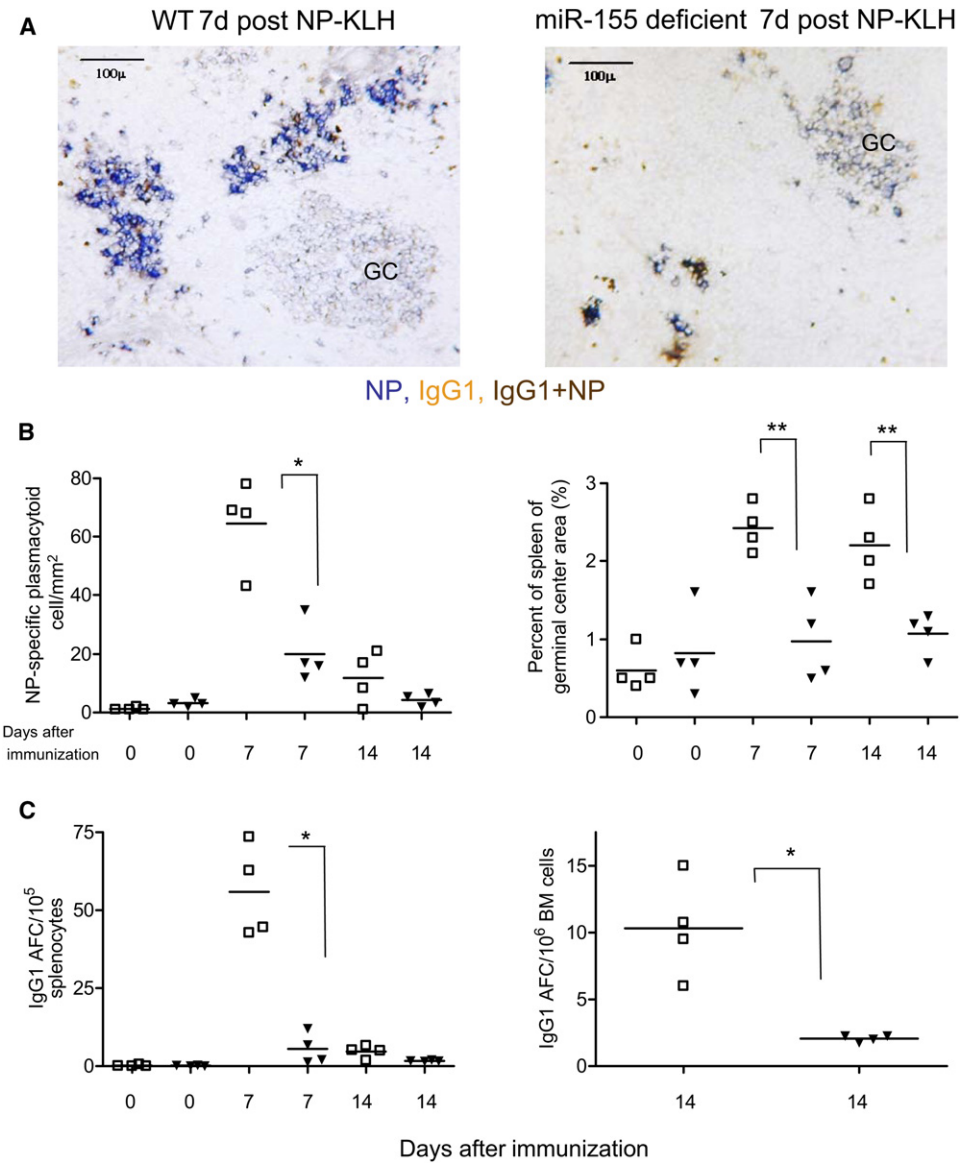

Figure 3. Impaired Extrafollicular and Germinal Center Response in the Absence of miR-155

(A) Immunohistochemical analysis of splenic sections from wild-type (WT) or miR-155 chimeric mice showing NP-binding cells (blue) and IgG1-positive cells (orange) on day 7 after immunization with NP-KLH.

(B) Wild-type (open squares) or miR-155-deficient (filled triangles) chimeras were immunized with NP-KLH. The graph on the left shows the number of NP-specific extrafollicular plasmacytoid cells per mm^2 of spleen section. The graph on the right shows the percentage of splenic section occupied by germinal centers.

(C) ELISPOT analysis of splenic NP-specific IgG1 AFC (left) or bone-marrow NP-specific IgG1 AFC (right).

(B and C) Each symbol represents one mouse and the horizontal bar corresponds to the media. Statistical analysis was performed by one-way ANOVA. *$p < 0.05$; **$p < 0.001$. In (B), no significance difference ($p > 0.05$) was observed when comparing miR-155-deficient NP-specific extrafollicular plasmacytoid cells per mm^2 at day 0 with day 7 or day 14. Similar experiments were repeated 2–3 times.

germinal centers resulting in the production of high-affinity antibodies by plasma cells and generation of memory B cells. Examination of naive miR-155-deficient μMT chimeric mice reveals no overt abnormality in the structure of the white pulp (data not shown). However, after immunization with NP-KLH, the extrafollicular response in miR-155-deficient μMT chimeric mice was severely impaired. This was reflected by a significant reduction in the number of NP-specific plasmacytoid cells (plasmablasts and or plasma cells) 7 days after immunization ($p < 0.05$; Figures 3A and 3B). By day 14, the number of NP-specific plasmacytoid cells had fallen, as expected, in the wild-type chimeric mice to 10% of their number at day 7. In the miR-155-deficient μMT chimeric mice, the numbers of NP-specific plasma cells had fallen to numbers that were not significantly different from those in nonimmunized chimeras

($p > 0.05$; Figure 3B). Kinetic analysis of the frequency of NP-specific IgG1 antibody-forming cells (AFC) in the spleen, measured by enzyme-linked immunosorbent spot (ELISPOT), mirrored the emergence and disappearance of NP-specific plasmacytoid cells (Figure 3C). Moreover, the frequency of NP-specific IgG1 AFCs was significantly reduced in the absence of miR-155 ($p < 0.05$; Figure 3C). The average spot size was similar to wild-type cells (145 ± 24 versus 141 ± 17, n = 4, mean ± SE), suggesting that miR-155 does not regulate secretion from plasmacytoid cells. Taken together, these results suggest that miR-155 regulates the output of antibodies produced in extrafollicular responses.

Analysis of the GC response showed that NP-specific GC were formed at day 7 in the miR-155-deficient, μMT-deficient chimeric mice (Figure 3A). However, the areas occupied by miR-155-deficient GCs were significantly smaller than those of wild-type mice ($p < 0.001$; Figures 3A and 3B). Similar results were observed at day 14 (Figure 3B), in agreement with a recent report (Thai et al., 2007). Antigen-specific plasma cells originating from the GC reaction preferentially migrate to the bone marrow where they reside for extended periods. We found that the frequency of NP-specific IgG1 AFC in the bone marrow 14 days after immunization was significantly reduced in the chimeric mice with miR-155-deficient B cells compared to those with WT B cells ($p < 0.05$; Figure 3C). Reduced switched antibody production by miR-155-deficient B cells is therefore a consequence of lowered numbers of switched plasma cells arising from the extrafollicular and the GC responses.

Impaired Memory Response in the Absence of miR-155 Is B Cell Autonomous

Secondary immunization of miR-155-deficient germline mice yielded reduced production of antigen-specific antibodies of low affinity (Figures 1B–1E). To assess intrinsic defects of miR-155-deficient memory B cells, we used the adoptive transfer method, because B cells influence T helper cell function and T cell memory (Linton et al., 2000, 2003; van Essen et al., 2000) and T cells, in turn, influence B cell memory function. $B220^+$ cells were purified from the spleens of WT, μMT chimeric or miR-155-deficient μMT chimeras previously immunized with NP-KLH in alum and mixed with KLH-primed T cells from C57BL/6 mice. The mixed cells were then transferred into *Rag2*$^{-/-}$ *Il2rg*$^{-/-}$ double-deficient mice and boosted with soluble NP-KLH. The titers of anti-NP IgG1 antibodies were below detection when the mice were not immunized, suggesting no contamination by long-lived AFC in transferred B cells (Figure 4). Also, NP-IgG1 titers from mice that received T cells only were below the limit of detection, suggesting no contamination with wild-type antigen-specific B cells (Figure 4). As observed in the primary response, we found reduced amounts of NP-specific IgG1 antibodies (Figures 4A and 4B) and impaired affinity maturation (Figure 4D). Thus, memory B cell function is regulated by miR-155 in a B cell-autonomous manner. To assess whether miR-155 is required for the generation and/or maintenance of memory B cells, we identified by FACS antigen-specific switched memory B cells 42 days after immunization with NP-KLH. At this time point, a stable population of $IgG1^+$, NP^+, $B220^+$ is found in the spleen (Blink et al., 2005). We observed a reduced proportion of switched memory cells in the absence of miR-155 (Figure 4E), suggesting that miR-155 may regulate the generation or maintenance of memory B cells.

Normal Rate of Somatic Hypermutation and Class Switch Recombination in miR-155-Deficient B Cells

Impaired production of high-affinity antibodies and reduced amounts of switched antibodies can result from dysfunction of the machinery for somatic hypermutation (SHM) and class switch recombination (CSR). To assess whether miR-155 was required for somatic hypermutation, we compared the frequency and pattern of mutations between wild-type and *miR-155*$^{-/-}$ mice in a system that is not biased by selection. This was achieved by sequencing the intronic V_HJ558-J_H rearrangement-flanking regions from germinal center B cells obtained from Peyer's patches (Jolly et al., 1997). Our analysis showed no significant difference in the frequency of mutations between wild-type and miR-155-deficient B cells ($p = 0.4$; Figure 5A). Moreover, no difference in the pattern of nucleotide substitutions was observed between wild-type and miR-155-deficient B cells (Figure 5A). We conclude that miR-155 does not regulate the machinery for SHM.

To examine CSR to IgG1, we used the well-characterized in vitro system of culturing B cells with LPS and IL-4 (Hodgkin et al., 1996). After culture with LPS and IL-4, miR-155-deficient B cells produced reduced IgG1 (Rodriguez et al., 2007). Defective secretion of IgG1 was accompanied by a reduction in the proportion of cells expressing IgG1 on the cell surface (Figure S1 in the Supplemental Data available online). Combinations of CD40 with IL-4 or IL-5 yielded similar results (Figure S1B). By contrast, the number of CD138-positive cells was only marginally impaired, consistent with normal IgM secretion (Figure S1B). This inhibition was not reflected in a failure of B cells to proliferate, as judged by incorporation of radioactive thymidine with a variety of stimuli (Rodriguez et al., 2007; also Figure S1A). We next quantified the expression of activation-induced cytidine deaminase (*Aicda*) mRNA, because this enzyme regulates CSR, but we found this was not reduced in the absence of miR-155 (Figure 5B). We also found similar expression of μ and γ1 encoding sterile transcripts as well as γ1 encoding post-switch circle transcripts in miR-155-deficient and wild-type B cells (Figure 5C). Thus, the failure of miR-155-deficient B cells to generate high-affinity switched antibodies appears not to be due to a defect in SHM or CSR but more likely to a defect in the differentiation or survival of plasmablasts.

We examined whether the reduction in the number of $IgG1^+$ cells after in vitro differentiation of miR-155-deficient B cells with LPS and IL-4 reflected defective survival. bcl-2 promotes survival of lymphocytes both in vivo and in vitro (Vaux, 1993), so we tested whether the number

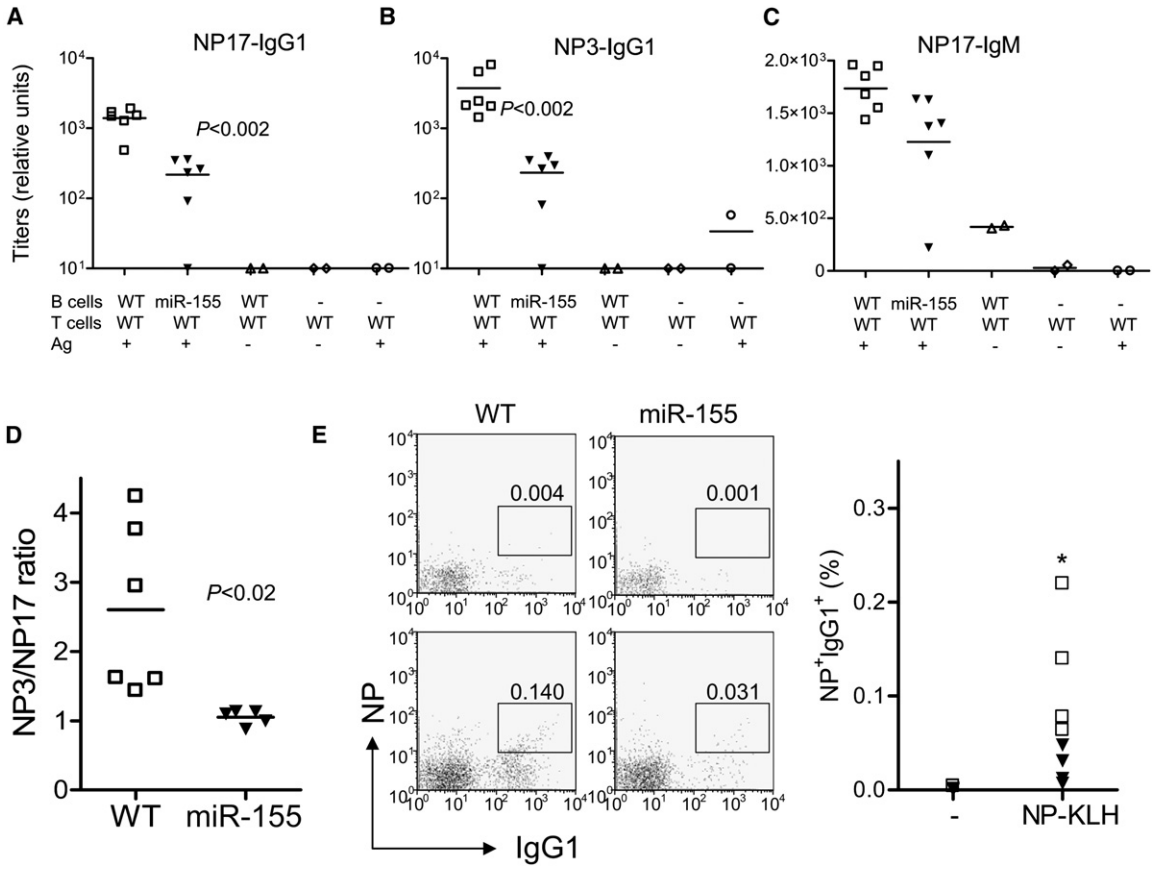

Figure 4. The Defective Memory Response in miR-155-Deficient Mice Is B Cell Intrinsic

NP-primed B cells from wild-type (WT) or miR-155-deficient (miR-155) chimeras were mixed with wild-type carrier-primed T cells and transferred into *Rag2*$^{-/-}$ *Il2rg*$^{-/-}$ mice. Subsequently, recipient mice were immunized with soluble NP-KLH, and 1 week later, antigen-specific IgM and IgG1 were measured. Control groups are indicated.

(A and B) Titers of IgG1 anti-NP measured with NP_{17}-BSA (A) or NP_3-BSA (B).

(C) Titers of IgM anti-NP with NP_{17}-BSA.

(D) Ratio of the IgG1 titers detected with NP_3-BSA to those with NP_{17}-BSA. Each symbol represents an individual mouse and horizontal bars indicate the average. The indicated p values were calculated by Student's t test.

(E) Frequency of memory B cells after 42 days of immunization with NP-KLH. Red blood cell-depleted splenic cells were gated as B220$^+$, CD4$^-$, CD8$^-$, IgM$^-$, IgD$^-$, Gr-1$^-$, F4/80$^-$, PI$^-$, and analyzed for the expression of NP and IgG1. Dot plots correspond to a representative example of a mouse of each genotype. The top panel corresponds to nonimmunized mice, the bottom panel to NP-KLH-immunized mice. The boxes indicate the frequency of NP$^+$, IgG1$^+$ cells. The graph summarizes the results of four mice of each genotype: open squares correspond to wild-type, filled triangles to miR-155-deficient mice. A significance reduction in the proportion of NP$^+$IgG1$^+$ cells after immunization was observed in the absence of miR-155 ($p = 0.03$, by Student's t test).

of IgG1$^+$ cells could be rescued by exogenous expression of bcl-2. To this end, miR-155-deficient B cells were transduced with a retrovirus expressing bcl-2 with an IRES-GFP reporter to enable the identification of infected cells. The results indicate that bcl-2 was unable to rescue the defect (Figure S2).

Genome-wide Analysis of Gene Expression Shows Enrichment of miR-155 Binding Sites in mRNA Upregulated in *miR-155*$^{-/-}$ B Cells

Our results thus far indicate that miR-155 is required for the maintenance and/or differentiation of IgG-switched cells. To analyze how the absence of miR-155 affects the global gene-expression program underlying B cell differentiation, we compared gene expression in wild-type and miR-155-deficient B cells treated with LPS and IL-4. Kinetic analysis indicates that *Bic* and miR-155 expression peaks at 24 hr after stimulation with LPS and IL-4 (Figure S3). This time point was chosen because it allows the examination of gene expression before the emergence of IgG1 cells. Because direct targets are predicted to have higher expression in absence of miR-155, we expected them to be enriched among the genes upregulated in miR-155-deficient B cells.

A total of 101 protein coding genes were significantly increased in miR-155-deficient B cells whereas 84 were decreased in expression ($p < 0.05$). Among the deregulated genes are transcription factors, signaling molecules, adhesion molecules, and regulators of chemotaxis (Tables S1 and S2). Several groups have computationally

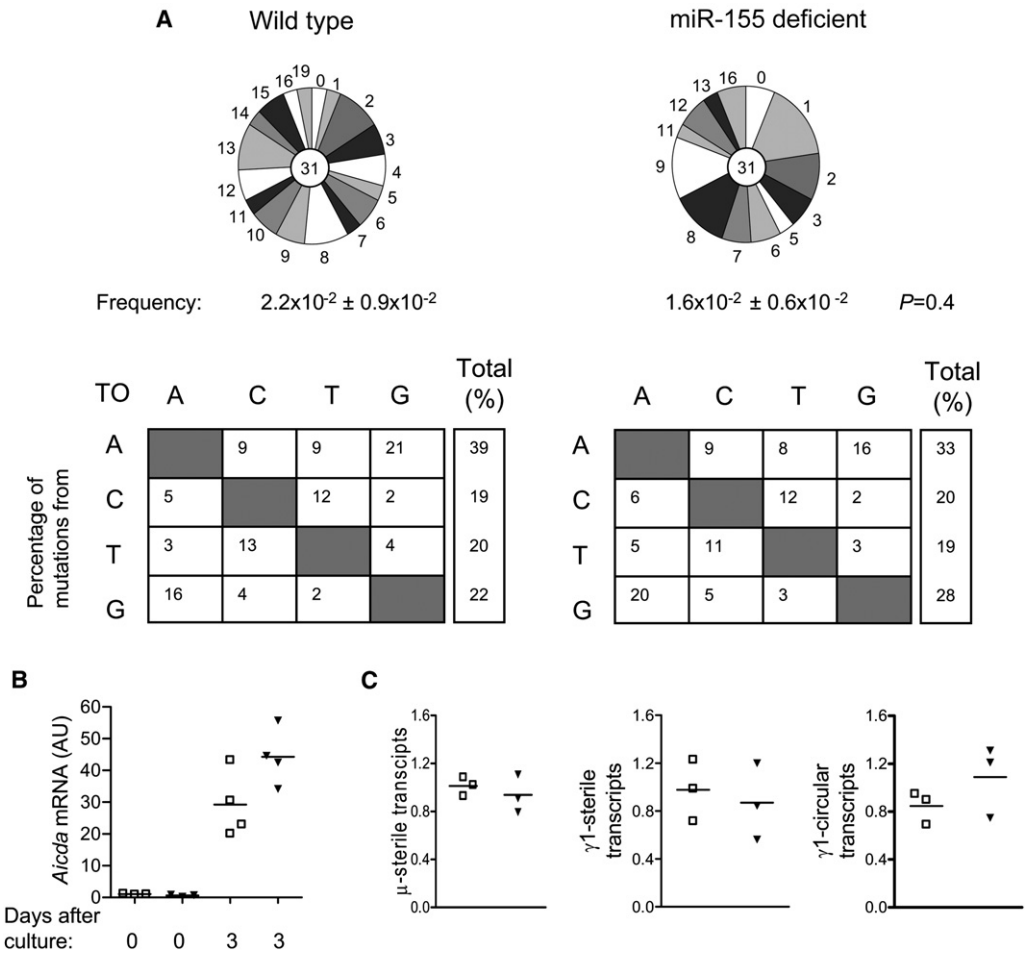

Figure 5. Hypermutation in miR-155-Deficient B Cells in Peyer's Patch GC Despite Impaired IgG1 Secretion

(A) Analysis of mutations in the intronic V_HJ558-J_H rearrangement-flanking region of wild-type and miR-155-deficient germinal center B cells purified from Peyer's Patches. Segment sizes in the pie charts are proportional to the number of sequences carrying the number of mutations indicated in the periphery of the charts. The total number of sequences analyzed is indicated in the center of the chart. The frequency of mutations is expressed as the mean ± SD for 3 mice per group, and the p value was calculated by Student's t test. The tables indicate the percentage nucleotide substitution. The total number of mutations was 275 for the wild-type and 196 for the miR-155-deficient mice.

(B and C) Splenic B cells were cultured with LPS+IL-4 for 3 days. Each symbol corresponds to B cells isolated from an individual mouse, the horizontal bar indicates the average, open squares correspond to wild-type B cells, and filled triangles to miR-155-deficient cells.

(B) Induction of *Aicda*.

(C) Expression of μ encoding sterile transcripts (left), γ1 encoding sterile transcripts (middle), and post-switch encoding γ1 circular transcripts (right). This experiment was repeated 2–3 times.

predicted miRNA targets based on perfect Watson-Crick complementarity of 6–8 nucleotides between the 5′ end of a miRNA and the 3′UTR of mRNAs (Brennecke et al., 2005; Doench and Sharp, 2004; Lai, 2002), a region of the miRNA referred to as the "seed." To test whether upregulated mRNAs in miR-155-deficient B cells may be direct miR-155 targets, we searched their 3′UTR for the presence of miR-155 seed matches. We found 97 upregulated transcripts with annotated 3′UTRs, 60 of which contain at least one seed match for miR-155 (Figure 6A; Table S2). As a control, we searched the upregulated gene set for seed matches for all mouse miRNAs present in miRBase 9.1 (Giraldez et al., 2006; Griffiths-Jones et al., 2006). Among all possible 6nt, 7nt, and 8nt seed sequences, only the enrichment of miR-155 matches was found to be statistically significant ($p = 4.3 \times 10^{-5}$, Figure 6B; Experimental Procedures). When performing a similar analysis with all possible hexamers, the miR-155 6nt seed was found to be the top-ranked hexamer (data not shown). These results demonstrate a highly significant enrichment of direct miR-155 targets among the mRNAs that were increased in abundance in miR-155-deficient B cells.

Pu.1 Is a Direct Target of miR-155, and Its Overexpression in Wild-Type B Cells Impairs the Emergence of IgG1-Switched Cells

Computationally predicted targets for miR-155 include transcription factors and regulators of cell differentiation and metabolism. Expression of *Aicda* was 1.6-fold increased in miR-155-deficient B cells (Table S2), a trend

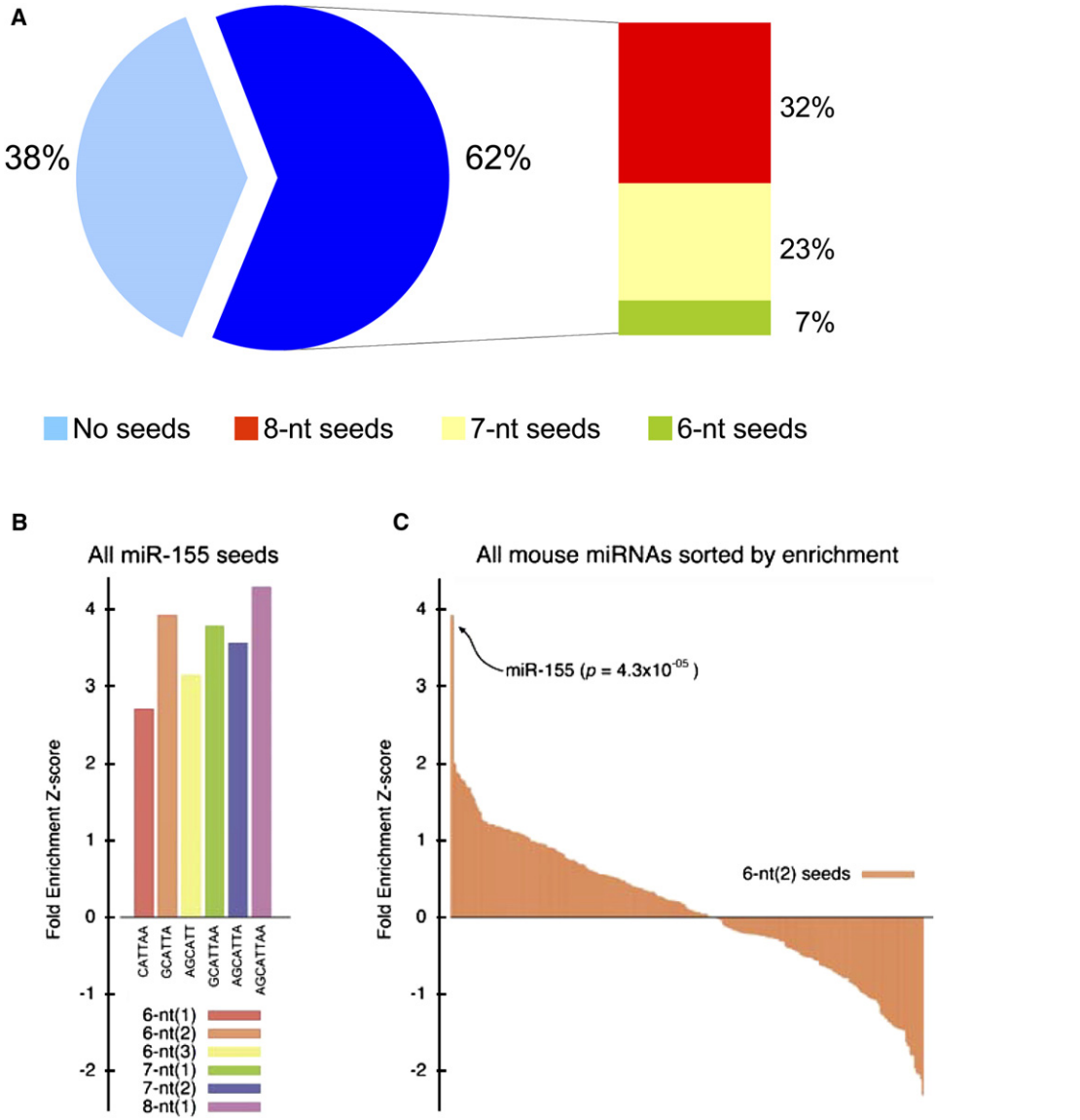

Figure 6. Enrichment for miR-155 Seeds in Genes Upregulated in miR155-Deficient B Cells

(A) Representation of miR-155 "seeds" in the group of upregulated genes in miR-155-deficient B cells. Genes were grouped according to their content of 6 nt seeds, 7 nt(1), 7 nt(2), or 8 nt miR-155 seeds and represented in a pie chart.

(B) Enrichment for 6 nt seeds, 7 nt(1), 7 nt(2), or 8 nt miR-155 seeds.

(C) Enrichment of mouse 5′miRNA seed sequences contained in the 3′UTRs of significantly upregulated genes. The p value for miR-155 is indicated.

we have also observed after 72 hr of in vitro culture with LPS and IL-4 (Figure 5B). We further validated the expression of five other genes upregulated in miR155-deficient B cells that contain miR-155 binding sites in their 3′UTRs, by quantitative PCR (Figure 7A). We focused our attention on *Sfpi1*, the gene encoding Pu.1, a member of the Ets domain-transcription factor family that plays a central role in many aspects of hematopoiesis. In B cells, Pu.1 is required at early developmental stages (McKercher et al., 1996; Scott et al., 1994) and has overlapping roles, in the regulation of B cell function, with another Ets family member SpiB (Garrett-Sinha et al., 1999). Pu.1 is expressed at low amounts in lymphocytes and was not readily detected by immunoblot of lysates from wild-type B cells. However, we could easily detect Pu.1 expressed in miR-155-deficient B cells (Figure 7B), consistent with Pu.1 being a direct target of miR-155. The 3′UTR of Pu.1 includes a phylogenetically conserved stretch of eight nucleotides perfectly complementary to the miR-155 seed region (Figure 7C, left). When the Pu.1 3′UTR was coupled to a luciferase reporter and cotransfected with miR155 mimics into 293T cells, we observed significant repression of the reporter ($p < 0.0001$; Figure 7C, right). The repression was alleviated when three nucleotides from the predicted binding site were mutated (Figure 7C, right), indicating that this binding site is functional. Taken

together, these results indicate that Pu.1 is a direct target of miR155. We next tested whether overexpression of Pu.1 recapitulated aspects of the phenotype caused by deletion of miR-155. To this end, we transduced wild-type B cells stimulated with LPS+IL-4 with a retroviral vector allowing bicistronic expression of Pu.1 and GFP. After 3 days, surface expression of IgG1 was determined in the fraction of B cells expressing Pu.1, which were identified on the basis of being GFP^+. We observed a reduction in the proportion of IgG1-expressing cells (Figure 7D), which resembled the in vitro phenotype of miR-155-deficient B cells (Figure S2). Similar results were observed when we measured intracellular expression of IgG1 (Figure 7E, left). The proportion of IgM-positive cells was accordingly increased when Pu.1 was overexpressed (Figure 7E, right). As with miR-155-deficient cells, the inability to switch was not due to altered cell division. Staining with the dye PKH26, which allowed tracking of cell divisions by GFP-expressing cells, showed a similar extent of division between wild-type cells transduced with GPF only expressing virus or GFP and Pu.1 (Figure 7F). The switching was specific to Pu.1, as shown by the fact that overexpression of another predicted target of miR-155, c-myb, resulted in impaired cell survival (data not shown). Taken together, our results suggest that miR-155 may affect the generation of $IgG1^+$ cells in vitro by regulating the expression of Pu.1.

DISCUSSION

Here we demonstrate that miR-155 is required for TI and TD responses, particularly the production of switched antibodies. Chimeric mice recapitulated all of the phenotypic alterations observed in the germline mice, and therefore B cells require miR-155 function in a cell-autonomous manner for the secretion of switched antibodies and affinity maturation in both primary and memory responses.

Our analysis of the primary TD response indicated the extrafollicular response was suppressed in miR-155-deficient B cells. This reduction was not due to defective proliferation, nor to reduced frequency of NP-binding B cell precursors (data not shown). In addition, we found reduced humoral responses after immunization with the TI antigens DNP-LPS and DNP-Ficoll (data not shown), two antigens that promote a robust extrafollicular response. It is thus possible that NP-specific cells are being recruited into the response, but miR-155 deficiency prevents most of these cells maturing into plasmablasts. Alternatively, there may be a high death rate among miR-155-deficient plasmablasts. In contrast to our current study, where immunization with haptenated proteins leads to normal IgM responses, infection of miR-155-deficient mice with attenuated *Salmonella* resulted in reduced secretion of antigen-specific IgM (Rodriguez et al., 2007). This difference may be due to the different responses these antigens elicit. Unlike NP-KLH, infection with *Salmonella* generates a massive T-dependent extrafollicular response that persists for up to 5 weeks (Cunningham et al., 2007). Furthermore, it is possible that reduction of IgM in the *Salmonella* infection is not B cell autonomous, because the experiment has been conducted only in germline mice.

The kinetics of formation of GCs was not affected by miR-155 deletion, despite a 50%–60% reduction in the size of the GCs. We found a 50% reduction in the proportion of GC B cells from Peyer's patches of miR-155-deficient mice (data not shown). The outcome of the GC response was also impaired, as shown by the fact that there were reduced numbers of antigen-specific IgG1 plasma cells within the bone marrow and impaired production of high-affinity antibody. The secondary IgM response of germline mice was defective, suggesting that low-affinity memory responses were impaired. Taken together, these data indicate that miR-155 may regulate the emergence or maintenance of memory cells.

SHM and CSR operate normally in the absence of miR-155, and therefore we suggest that miR-155-deficient B cells are likely able to class switch and hypermutate in vivo. The loss of affinity maturation in the presence of hypermutation suggests that there is a failure to select high-affinity B cells. This might reflect impaired signaling through the BCR or other receptors during selection and may partly explain the reduction in size of the GCs. In support of that, *BIC* is expressed upon BCR crosslinking (van den Berg et al., 2003), by a subset of germinal center B cells (van den Berg et al., 2003), and, in mice, upon CD40 stimulation (data not shown). Some limited selection must be occurring, because GC in the chimeras with miR-155-deficient B cells were small but persistent. Overexpression of bcl-2 can prolong survival but cannot provide differentiation signals. Thus, in vivo miR-155-deficient B cells may be receiving sufficient selection signals to survive, but still may be failing to receive, or respond to, signals that induce differentiation to plasma cells. Another contributing factor to the defective germinal center response in miR-155 may be reduced production of cytokines by B cells, as has been previously suggested (Thai et al., 2007). However, our histological analysis showed that the anatomy of the germinal centers (dark and light zones) was not affected by the absence of miR-155 in B cells (data not shown).

Our current model of plasma cell differentiation is based on the concerted action of several transcription factors (reviewed by Shapiro-Shelef and Calame, 2005). Our results show that miR-155 directly regulates the expression of Pu.1, and its overexpression impairs the emergence of IgG1-positive cells. It is currently unknown how Pu.1 may regulate terminal B cell differentiation, because no phenotype was observed in mice with B cells deficient in Pu.1 (Polli et al., 2005). It is worth noting that Pu.1 is highly expressed in germinal center B cells and is downregulated in post-germinal center cells (Cattoretti et al., 2006). Therefore, it is possible that miR-155 is required for the downregulation of Pu.1, and, in the absence of miR-155, excessive Pu.1 affects the output of the germinal center reaction.

Microarray analysis showed that deletion of a single miRNA in B cells causes deregulation of a large number of genes. Among genes that showed increased

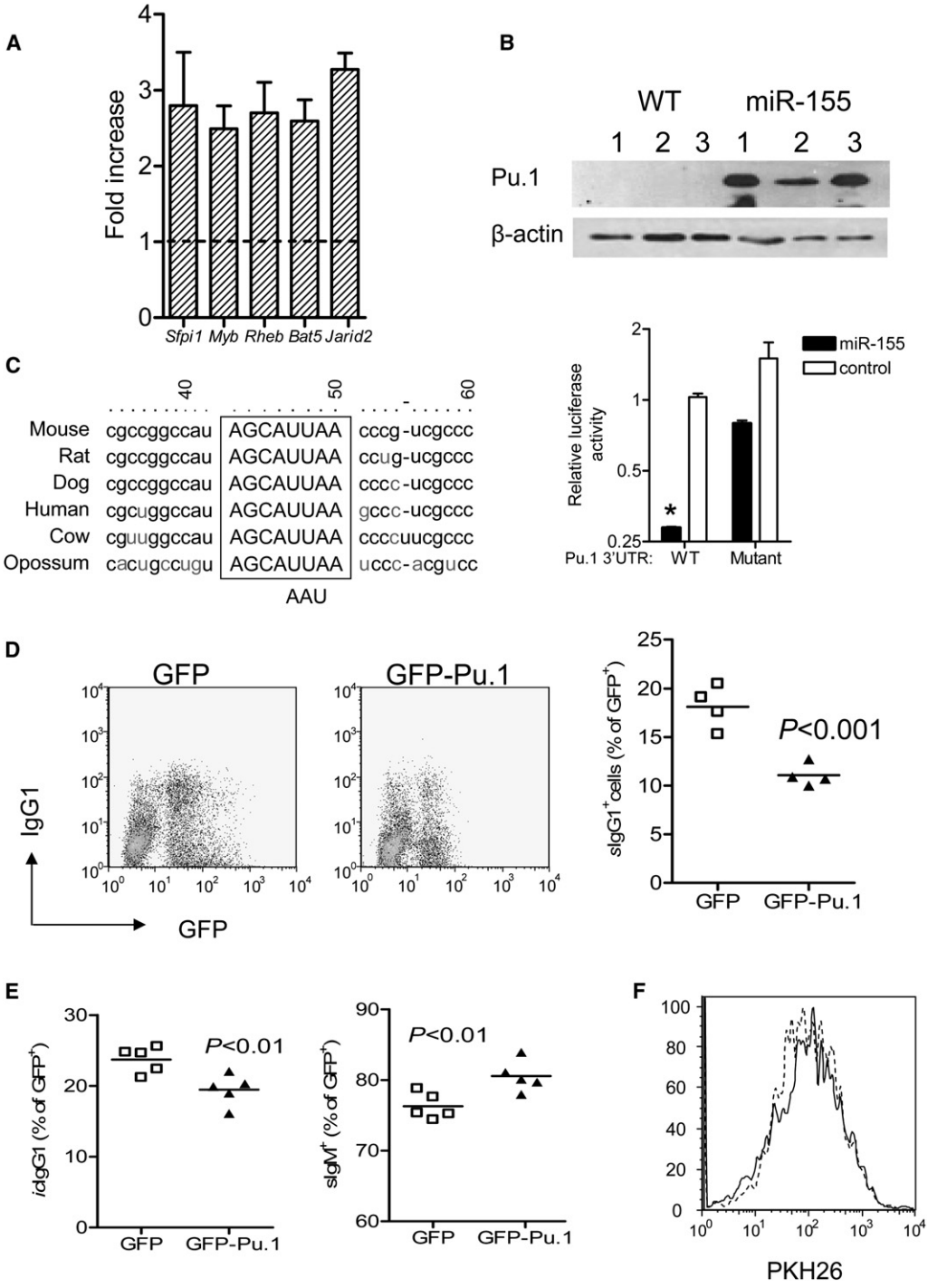

Figure 7. Pu.1 Is a Direct Target of miR155 and Its Overexpression in Wild-Type B Cells Results in a Reduction of IgG1-Switched Cells

(A) Expression of *Sfpi1*, *Myb, Rheb, Bat5*, and *Jarid2* was assessed by q-PCR. Data are represented as the increase in miR-155 relative to wild-type amounts set at 1 (n = 4). Error bars correspond to the standard error of the mean. For all genes, $p \leq 0.05$.

(B) Protein expression of Pu.1 from B cell cultures from 3 wild-type and 3 miR-155-deficient mice.

(C) Left panel, sequence alignment of part of the 3′UTR of PU.1 from different species. The 8 ntmiR155 binding site is boxed. The AAU sequence indicated below the alignment shows the mutagen derivative created to assess miR-155-dependent translational repression in the luciferase reporter assay. Wild-type (WT) or mutant Pu.1 (mutant) plasmid were cotransfected with miR-155 mimic (closed bars) or control miR-124a (open bars). The right panel shows a significant miR-155-specific repression of Pu.1 reporter. Results are presented as mean ± standard error of the mean for triplicate transfections. *$p < 0.0001$ in comparison with wild-type plasmid treated control mimic by Student's t test.

expression, more than half of them were predicted to be direct targets of miR-155. It is thus possible that the phenotypic alterations observed in miR-155-deficient mice are the result of deregulation of other targets in addition to Pu.1. Such a view is consistent with recent reports of the role of miR-181a in setting the threshold for T cell receptor signal transduction through the regulation of multiple phosphatases (Li et al., 2007) or in the regulation of cardiogenesis by miRNA-1-2 (Zhao et al., 2007). Elucidating how deregulation of Pu.1 contributes to the phenotype caused by deletion of miR-155 in vivo will be the next challenge.

EXPERIMENTAL PROCEDURES

Generation of Chimeric Mice and Immunization

miR-155-deficient mice (*Bic*^{m2} allele) were previously described (Rodriguez et al., 2007). For TI responses, *Rag2*$^{-/-}$ *Il2rg*$^{-/-}$ mice were irradiated (5.0 Gy) and reconstituted with 3 × 10^6 bone-marrow cells. For the generation of mixed chimeras, irradiated *Rag2*$^{-/-}$ *Il2rg*$^{-/-}$ mice received a mixture of 80% bone-marrow cells of μMT origin and 20% wild-type or miR-155-deficient cells. For TI responses, 25 μg of DNP-LPS was administered intraperitoneally. For TD responses, 100 μg of alum-precipitated NP-KLH (Biosearch Tech) was used.

Adoptive Transfer and Immunization

Splenic B cells were enriched by positive selection with B220 beads (Miltenyi Biotech) from either WT, μMT chimeras or miR-155-deficient μMT chimeras previously immunized with 100 μg of NP-KLH precipitated in alum. T cells were enriched by negative selection by MACS system (Miltenyi Biotech) from the spleens of C57BL/6 immunized with NP-KLH in alum. The mixture of separated B cells (5 × 10^6) and T cells (2.0 × 10^6) were i.v. injected into *Rag2*$^{-/-}$ *Il2rg*$^{-/-}$ mice and subsequently immunized with 50 μg of soluble NP-KLH.

ELISA and ELISPOT Assay

NP-specific AFC were detected with ELISPOT as previously described (Xiang et al., 2007). NP-specific antibodies were detected by ELISA as previously described, except that antibody end point titers were used as a measure of relative concentration.

Immunohistology

NP, IgG1 staining were detected as described previously (Cunningham et al., 2002; Luther et al., 1997). NP-binding cells were detected with NP conjugated to sheep IgG fraction. Biotinylated donkey anti-goat-Ig antibodies (Dako), which bind sheep Ig, were used as a conjugate to detect bound NP–sheep-Ig (Luther et al., 1997). The proportion of spleen sections occupied by germinal sections was determined by the point counting technique of Weible (Weibel, 1963). NP-specific plasmacytoid cells per mm^2 were counted at ×100 magnification with serial sweeps of each spleen section by means of a 1 cm^2 eyepiece graticule divided into 100 one mm^2 squares to define the section area being counted.

B Cell Stimulation and Quantitative PCR

B cells were purified by negative selection with the MACS system (Miltenyi Biotech) and stimulated with 10 μg/ml LPS (Sigma) and 20 ng/ml IL-4 (Peprotech) for 3 days. Subsequently, RNA was extracted with TRIzol (Invitrogen) and converted to cDNA. Controls without reverse transcriptase were included for all samples. *Aicda, Sfpi1, Myb, Bat5, Rheb, Jarid2* mRNA, and *Bic* mRNA were quantified with Taqman probes (Applied Biosystems) and normalized to the expression of β2M (Applied Biosystems). Expression of μ and γ1 encoding sterile transcripts and post-switch γ1 encoding circular transcripts were normalized with GADPH exactly as described (Reina-San-Martin et al., 2003).

SHM

Germinal center B cells were identified as and purified by FACS sorting. We analyzed somatic hypermutation by monitoring mutations in the intronic V_HJ558-J_H rearrangement-flanking region in germinal center B cells purified from Peyer's patches as described (Jolly et al., 1997). GC B cells were identified as B220$^+$CD95$^+$ PNA^{high} and purified by FACS sort from 4-month-old mice (C57BL/6).

Microarray Analysis

B cells from five wild-type and five miR-155-deficient mice were cultured with LPS and IL-4 for 24 hr as described above, and RNA was extracted with TRIzol. Gene-expression profiling was performed by hybridization to the mouse genome 430 2.0 Genechip arrays (Affymetrix) by Geneservice Ltd (Cambridge, UK). Genes with $p < 0.05$ and a fold expression difference $\geq |1.5|$ were selected for further analysis.

Computational miRNA Target Search and Calculation of Binding Site Frequencies in Mouse 3′UTRs

The method used to calculate miRNA binding site frequencies was essentially as described (Giraldez et al., 2006). Mouse miRNAs in miRbase registry Release 9.1 (Griffiths-Jones, 2004) were included in our analysis. The set of upregulated transcripts for which 3′UTR sequences could be obtained (test group) were examined for potential miRNA "seed" matches. The average number of seed sequences found in the test group per 1 kb of sequence was used to calculate seed "Observed Frequency" (F_obs) values. The seed "Genome Frequency" (F_genome) values were calculated from all mouse 3′UTRs present on the microarray and represent the average occurrence for any given seed sequence pattern per 1 kb of sequence. The "Fold Enrichment" (FE) value is calculated as: FE = log(F_obs/F_genome). To correct for low-count biases, those miRNAs whose 6nt(2) seed was present at less than 0.1 sites/kb in genomic 3′UTRs were removed from the analysis. To calculate the statistical significance of the FE for any seed, we randomly selected 10,000 sets with the same number of 3′UTR as the test group. From each one of these, FE_rand values were calculated and the mean and standard deviation (SD) were obtained. We can then describe any seed FE with a Z score = (FE – mean)/SD. These Z-scores are essentially "Fold Enrichment" scores that have been normalized, taking into account the enrichment variability of that particular seed in the genome. A p value was calculated for each Z score as well as an E value that takes into account the multiple numbers of seeds that we are testing.

Luciferase Assays

The *Sfpi1* 3′UTR was amplified from genomic DNA and inserted into the psiCheck-2 renilla luciferase reporter plasmid (Promega). This construct was used to derive a miR-155 "seed" mutant plasmid with the QuikChange Multi Site Mutagenesis Kit (Stratagene). The mutagenic primers used were sense, 5′-gaccccgccggccatagcaaatacccgtcgcc-3′, and antisense, 5′-ggcgacgggtatttgctatggccggcggggtc-3′. The

(D–F) Wild-type or miR-155-deficient B cells were cultured in the presence of LPS and IL-4. After 16 hr, cells were transduced with retrovirus expressing GFP or GFP and Pu.1 and cultured for 3 more days.
(D) Cultures were then stained for surface IgG1 expression. The left panel shows a representative example of cultures from one mouse transduced with each virus. The graph summarizes the results observed for cultures arising from four mice.
(E) Same as (D) except cells were stained for intracellular IgG1 (icIgG1) expression (left) or surface IgM (sIgM, right).
(F) Before culture, B cells were stained with PKH26 to follow proliferation. Representative histograms gated on GFP$^+$ cells for B cells transduced with GFP virus (black line) or GFP-Pu.1 (dashed line) are shown. This experiment was repeated 2–4 times.

correctness of all plasmids was confirmed by sequencing. Reporter assays were performed in 293T cells cotransfected in triplicates with Lipofectamine 2000 (Invitrogen) with test plasmid (3′UTR Pu.1 wild-type or mutant) along with either murine miR-155 mimic or miR-124a control (Dharmacon) at a final concentration of 40 nM. Firefly luciferase was used as a normalization control. Reporter activity was detected 24 hr after transfection with the Dual-Glo Luciferase Assay System (Promega). Expression values were normalized against the average value for the corresponding plasmid as in Rodriguez et al. (2007).

Retroviral Infection and FACS Analysis

Stable cell lines with bicistronic expression of bcl-2 and GFP or GFP alone were kindly provided by D. Wang (Wen et al., 2003). Retroviral control and GFP/Pu.1-expressing vectors were kindly provided by R. DeKoter (DeKoter and Singh, 2000). In this case, viral supernatants were collected 48 hr after transiently transfecting PlatE cells. Purified B cells were cultured with LPS and IL-4 as described above. After 16 hr, cell supernatant was removed and cells were resuspended in viral supernatant supplemented with 6 μg/ml of polybrene, LPS, and IL-4 and centrifuged for 30 min at 2500 rpm at room temperature. Cells were returned to 37°C, and the following day, supernatant was removed and cells were recultured in LPS and IL-4 until analyzed by FACS. Cultured cells were stained with the following antibodies: anti-Syndecan 1 (CD138), 281.2 (BD); anti-IgG1, A85-1; and anti-IgM, goat polyclonal (Jackson Laboratories). For intracellular staining, cells were fixed for 20 min with Cytofix-cytoperm (BD) and stained in Perm-wash solution (BD). Data were collected with FACscaliber or LSRII (BD) and analyzed with Flowjo (treestar).

Proliferation

The following B cell stimuli were used at the indicated concentrations: anti-IgM $F(ab)_2$ fragment, 5 μg/ml; anti-CD40 (3/23 clone), 10 μg/ml; mIL-4 (Peprotech), 20 ng/ml; mIL-5 (Sigma), 25 ng/ml. B cell proliferation was measured after addition of $[^3H]$thymidine for the final 16 hr of culture.

Bic and miR-155 Expression

Expression of *Bic* was measured by quantitative PCR as previously described (Rodriguez et al., 2007). miR-155 expression was determined by northern blot as previously described (Rodriguez et al., 2007).

Statistical Analysis

Statistical analysis was performed with two-tailed Student's t test or one-way or two-ways ANOVA, as indicated in the figures legends, with GraphPad Prism 4 or Graphpad InStat 3 software.

Supplemental Data

Three figures and two tables are available at http://www.immunity.com/cgi/content/full/27/6/847/DC1/.

ACKNOWLEDGMENTS

We are grateful to S.E. Bell, K. Welch, and S. Andrews for technical assistance and SABU and SAU staff and K. Okkenhaug and D. Hodson for critical reading of the manuscript. E.V. is supported by a Babraham Institute Career Progression Fellowship, and M.T. is supported by the MRC and the Biotechnology and Biological Sciences Research Council.

Received: April 18, 2007
Revised: September 14, 2007
Accepted: October 29, 2007
Published online: December 6, 2007

REFERENCES

Bartel, D.P. (2004). MicroRNAs: genomics, biogenesis, mechanism, and function. Cell *116*, 281–297.

Blink, E.J., Light, A., Kallies, A., Nutt, S.L., Hodgkin, P.D., and Tarlinton, D.M. (2005). Early appearance of germinal center-derived memory B cells and plasma cells in blood after primary immunization. J. Exp. Med. *201*, 545–554.

Brennecke, J., Stark, A., Russell, R.B., and Cohen, S.M. (2005). Principles of microRNA-target recognition. PLoS Biol. *3*, e85. 10.1371/journal.pbio.0030085.

Cattoretti, G., Shaknovich, R., Smith, P.M., Jack, H.M., Murty, V.V., and Alobeid, B. (2006). Stages of germinal center transit are defined by B cell transcription factor coexpression and relative abundance. J. Immunol. *177*, 6930–6939.

Cobb, B.S., Nesterova, T.B., Thompson, E., Hertweck, A., O'Connor, E., Godwin, J., Wilson, C.B., Brockdorff, N., Fisher, A.G., Smale, S.T., and Merkenschlager, M. (2005). T cell lineage choice and differentiation in the absence of the RNase III enzyme Dicer. J. Exp. Med. *201*, 1367–1373.

Cobb, B.S., Hertweck, A., Smith, J., O'Connor, E., Graf, D., Cook, T., Smale, S.T., Sakaguchi, S., Livesey, F.J., Fisher, A.G., and Merkenschlager, M. (2006). A role for Dicer in immune regulation. J. Exp. Med. *203*, 2519–2527.

Costinean, S., Zanesi, N., Pekarsky, Y., Tili, E., Volinia, S., Heerema, N., and Croce, C.M. (2006). Pre-B cell proliferation and lymphoblastic leukemia/high-grade lymphoma in E{micro}-miR155 transgenic mice. Proc. Natl. Acad. Sci. USA *103*, 7024–7029.

Cunningham, A.F., Fallon, P.G., Khan, M., Vacheron, S., Acha-Orbea, H., MacLennan, I.C., McKenzie, A.N., and Toellner, K.M. (2002). Th2 activities induced during virgin T cell priming in the absence of IL-4, IL-13, and B cells. J. Immunol. *169*, 2900–2906.

Cunningham, A.F., Gaspal, F., Serre, K., Mohr, E., Henderson, I.R., Scott-Tucker, A., Kenny, S.M., Khan, M., Toellner, K.M., Lane, P.J., and MacLennan, I.C. (2007). *Salmonella* induces a switched antibody response without germinal centers that impedes the extracellular spread of infection. J. Immunol. *178*, 6200–6207.

DeKoter, R.P., and Singh, H. (2000). Regulation of B lymphocyte and macrophage development by graded expression of PU.1. Science *288*, 1439–1441.

Doench, J.G., and Sharp, P.A. (2004). Specificity of microRNA target selection in translational repression. Genes Dev. *18*, 504–511.

Eis, P.S., Tam, W., Sun, L., Chadburn, A., Li, Z., Gomez, M.F., Lund, E., and Dahlberg, J.E. (2005). Accumulation of miR-155 and *BIC* RNA in human B cell lymphomas. Proc. Natl. Acad. Sci. USA *102*, 3627–3632.

Garrett-Sinha, L.A., Su, G.H., Rao, S., Kabak, S., Hao, Z., Clark, M.R., and Simon, M.C. (1999). PU.1 and Spi-B are required for normal B cell receptor-mediated signal transduction. Immunity *10*, 399–408.

Giraldez, A.J., Mishima, Y., Rihel, J., Grocock, R.J., Van Dongen, S., Inoue, K., Enright, A.J., and Schier, A.F. (2006). Zebrafish MiR-430 promotes deadenylation and clearance of maternal mRNAs. Science *312*, 75–79.

Griffiths-Jones, S. (2004). The microRNA registry. Nucleic Acids Res. *32*, D109–D111.

Griffiths-Jones, S., Grocock, R.J., van Dongen, S., Bateman, A., and Enright, A.J. (2006). miRBase: microRNA sequences, targets and gene nomenclature. Nucleic Acids Res. *34*, D140–D144.

Haasch, D., Chen, Y.W., Reilly, R.M., Chiou, X.G., Koterski, S., Smith, M.L., Kroeger, P., McWeeny, K., Halbert, D.N., Mollison, K.W., et al. (2002). T cell activation induces a noncoding RNA transcript sensitive to inhibition by immunosuppressant drugs and encoded by the proto-oncogene, *BIC*. Cell. Immunol. *217*, 78–86.

Herzenberg, L.A., Black, S.J., Tokuhisa, T., and Herzenberg, L.A. (1980). Memory B cells at successive stages of differentiation. Affinity maturation and the role of IgD receptors. J. Exp. Med. *151*, 1071–1087.

Hodgkin, P.D., Lee, J.H., and Lyons, A.B. (1996). B cell differentiation and isotype switching is related to division cycle number. J. Exp. Med. *184*, 277–281.

Huntington, N.D., Xu, Y., Puthalakath, H., Light, A., Willis, S.N., Strasser, A., and Tarlinton, D.M. (2006). CD45 links the B cell receptor with cell survival and is required for the persistence of germinal centers. Nat. Immunol. *7*, 190–198.

Jolly, C.J., Klix, N., and Neuberger, M.S. (1997). Rapid methods for the analysis of immunoglobulin gene hypermutation: application to transgenic and gene targeted mice. Nucleic Acids Res. *25*, 1913–1919.

Lagos-Quintana, M., Rauhut, R., Yalcin, A., Meyer, J., Lendeckel, W., and Tuschl, T. (2002). Identification of tissue-specific microRNAs from mouse. Curr. Biol. *12*, 735–739.

Lai, E.C. (2002). Micro RNAs are complementary to 3′ UTR sequence motifs that mediate negative post-transcriptional regulation. Nat. Genet. *30*, 363–364.

Li, Q.J., Chau, J., Ebert, P.J., Sylvester, G., Min, H., Liu, G., Braich, R., Manoharan, M., Soutschek, J., Skare, P., et al. (2007). miR-181a is an intrinsic modulator of T cell sensitivity and selection. Cell *129*, 147–161.

Linton, P.J., Harbertson, J., and Bradley, L.M. (2000). A critical role for B cells in the development of memory CD4 cells. J. Immunol. *165*, 5558–5565.

Linton, P.J., Bautista, B., Biederman, E., Bradley, E.S., Harbertson, J., Kondrack, R.M., Padrick, R.C., and Bradley, L.M. (2003). Costimulation via OX40L expressed by B cells is sufficient to determine the extent of primary CD4 cell expansion and Th2 cytokine secretion in vivo. J. Exp. Med. *197*, 875–883.

Luther, S.A., Gulbranson-Judge, A., Acha-Orbea, H., and MacLennan, I.C. (1997). Viral superantigen drives extrafollicular and follicular B cell differentiation leading to virus-specific antibody production. J. Exp. Med. *185*, 551–562.

McKercher, S.R., Torbett, B.E., Anderson, K.L., Henkel, G.W., Vestal, D.J., Baribault, H., Klemsz, M., Feeney, A.J., Wu, G.E., Paige, C.J., and Maki, R.A. (1996). Targeted disruption of the PU.1 gene results in multiple hematopoietic abnormalities. EMBO J. *15*, 5647–5658.

Metzler, M., Wilda, M., Busch, K., Viehmann, S., and Borkhardt, A. (2004). High expression of precursor microRNA-155/BIC RNA in children with Burkitt lymphoma. Genes Chromosomes Cancer *39*, 167–169.

Muljo, S.A., Ansel, K.M., Kanellopoulou, C., Livingston, D.M., Rao, A., and Rajewsky, K. (2005). Aberrant T cell differentiation in the absence of Dicer. J. Exp. Med. *202*, 261–269.

Neilson, J.R., Zheng, G.X., Burge, C.B., and Sharp, P.A. (2007). Dynamic regulation of miRNA expression in ordered stages of cellular development. Genes Dev. *21*, 578–589.

O'Connell, R.M., Taganov, K.D., Boldin, M.P., Cheng, G., and Baltimore, D. (2007). MicroRNA-155 is induced during the macrophage inflammatory response. Proc. Natl. Acad. Sci. USA *104*, 1604–1609.

Polli, M., Dakic, A., Light, A., Wu, L., Tarlinton, D.M., and Nutt, S.L. (2005). The development of functional B lymphocytes in conditional PU.1 knock-out mice. Blood *106*, 2083–2090.

Reina-San-Martin, B., Difilippantonio, S., Hanitsch, L., Masilamani, R.F., Nussenzweig, A., and Nussenzweig, M.C. (2003). H2AX is required for recombination between immunoglobulin switch regions but not for intra-switch region recombination or somatic hypermutation. J. Exp. Med. *197*, 1767–1778.

Rodriguez, A., Vigorito, E., Clare, S., Warren, M.V., Couttet, P., Soond, D.R., van Dongen, S., Grocock, R.J., Das, P.P., Miska, E.A., et al. (2007). Requirement of bic/microRNA-155 for normal immune function. Science *316*, 608–611.

Scott, E.W., Simon, M.C., Anastasi, J., and Singh, H. (1994). Requirement of transcription factor PU.1 in the development of multiple hematopoietic lineages. Science *265*, 1573–1577.

Shapiro-Shelef, M., and Calame, K. (2005). Regulation of plasma-cell development. Nat. Rev. Immunol. *5*, 230–242.

Tam, W., Ben-Yehuda, D., and Hayward, W.S. (1997). *bic*, a novel gene activated by proviral insertions in avian leukosis virus-induced lymphomas, is likely to function through its noncoding RNA. Mol. Cell. Biol. *17*, 1490–1502.

Thai, T.H., Calado, D.P., Casola, S., Ansel, K.M., Xiao, C., Xue, Y., Murphy, A., Frendewey, D., Valenzuela, D., Kutok, J.L., et al. (2007). Regulation of the germinal center response by microRNA-155. Science *316*, 604–608.

van den Berg, A., Kroesen, B.J., Kooistra, K., de Jong, D., Briggs, J., Blokzijl, T., Jacobs, S., Kluiver, J., Diepstra, A., Maggio, E., and Poppema, S. (2003). High expression of B-cell receptor inducible gene *BIC* in all subtypes of Hodgkin lymphoma. Genes Chromosomes Cancer *37*, 20–28.

van Essen, D., Dullforce, P., Brocker, T., and Gray, D. (2000). Cellular interactions involved in Th cell memory. J. Immunol. *165*, 3640–3646.

Vaux, D.L. (1993). Toward an understanding of the molecular mechanisms of physiological cell death. Proc. Natl. Acad. Sci. USA *90*, 786–789.

Victoratos, P., Lagnel, J., Tzima, S., Alimzhanov, M.B., Rajewsky, K., Pasparakis, M., and Kollias, G. (2006). FDC-specific functions of p55TNFR and IKK2 in the development of FDC networks and of antibody responses. Immunity *24*, 65–77.

Weibel, E.R. (1963). Principles and methods for the morphometric study of the lung and other organs. Lab. Invest. *12*, 131–155.

Wen, R., Chen, Y., Xue, L., Schuman, J., Yang, S., Morris, S.W., and Wang, D. (2003). Phospholipase Cgamma2 provides survival signals via Bcl2 and A1 in different subpopulations of B cells. J. Biol. Chem. *278*, 43654–43662.

Xiang, Z., Cutler, A.J., Brownlie, R.J., Fairfax, K., Lawlor, K.E., Severinson, E., Walker, E.U., Manz, R.A., Tarlinton, D.M., and Smith, K.G. (2007). FcgammaRIIb controls bone marrow plasma cell persistence and apoptosis. Nat. Immunol. *8*, 419–429.

Zhao, Y., Ransom, J.F., Li, A., Vedantham, V., von Drehle, M., Muth, A.N., Tsuchihashi, T., McManus, M.T., Schwartz, R.J., and Srivastava, D. (2007). Dysregulation of cardiogenesis, cardiac conduction, and cell cycle in mice lacking miRNA-1–2. Cell *129*, 303–317.

Accession Numbers

Microarray data for the data presented in this paper have been deposited in the ArrayExpress database with accession number E-MEXP-1325.